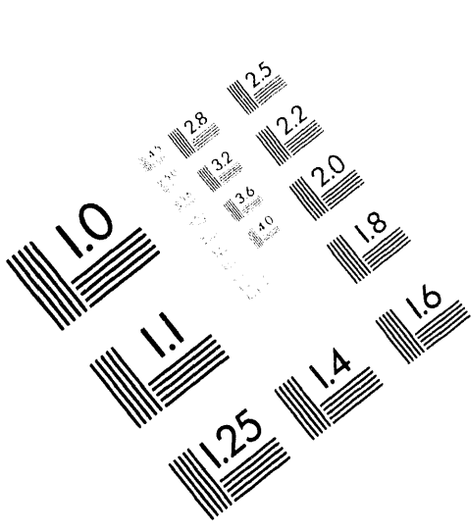

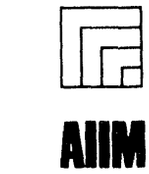

Association for Information and Image Management

1100 Wayne Avenue, Suite 1100
Silver Spring, Maryland 20910

301/587-8202

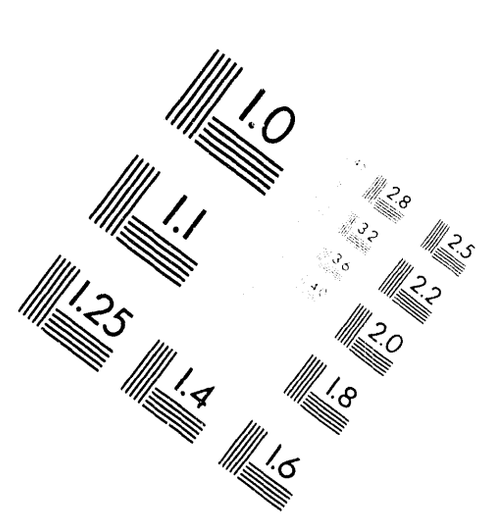

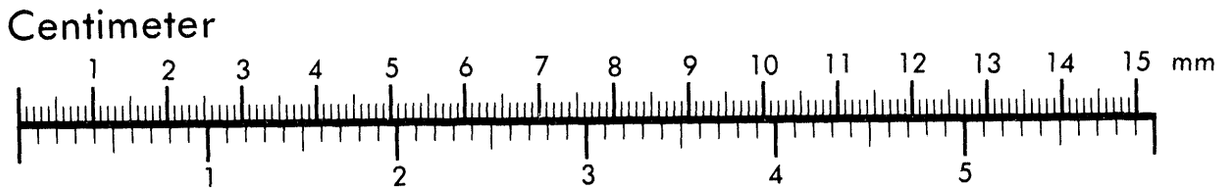

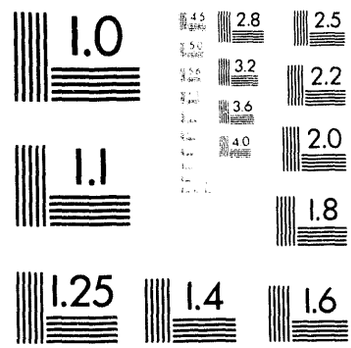

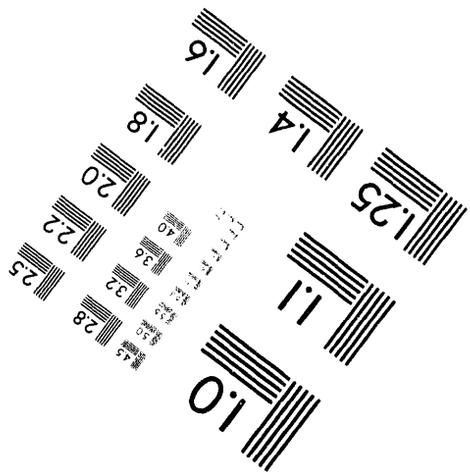

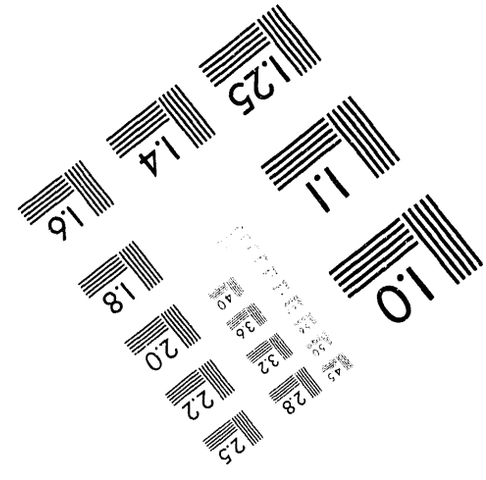

MANUFACTURED TO AIIM STANDARDS
BY APPLIED IMAGE, INC.

1 of 1

2

MAGNETIC FIELD INDUCED MINIGAP IN DOUBLE QUANTUM WELLS

J. A. SIMMONS, N. E. HARFF,* S. K. LYO, AND J. F. KLEM
Sandia National Laboratories, P. O. Box 5800,
Albuquerque, New Mexico 87185 USA

ABSTRACT

We report the discovery of a partial energy gap, or minigap, in strongly coupled double quantum wells (QWs), due to an anticrossing of the two QW dispersion curves. The anticrossing and minigap are induced by an in-plane magnetic field $B_{||}$, and give rise to large distortions in the Fermi surface and density of states, including a Van Hove singularity. Sweeping $B_{||}$ moves the minigap through the Fermi level, with the upper and lower gap edges producing a sharp maximum and minimum in the low-temperature in-plane conductance, in agreement with theoretical calculations. The gap energy may be directly determined from the data.

1. Introduction

Applying an in plane magnetic field $B_{||}$ to a double quantum well (QW) causes the canonical momenta k of electrons in one QW to be shifted relative to those in the other. The shift is given by $\Delta k_y = edB/\hbar$, where d is the distance between the two electron layers, and direction y is normal to both the growth and $B_{||}$ directions. Recent studies[1,2] have shown this to have a strong effect on interwell tunneling, due to the conservation of k. Little attention, however, has been paid to the effect of this shift on the in-plane conductance $G_{||}$.[3] This is of interest since the shifted dispersion curves of two strongly coupled QWs can be expected to produce an anticrossing, resulting in a large minigap. At sufficiently high B|| the minigap can be made to pass through the Fermi level. Under these conditions the DQW has a multi-component Fermi surface whose shape and topology is tunable by B||.[4] Our data show the presence of this minigap, and demonstrate that the electronic density of states and group velocities are dramatically distorted near its edges, producing the observed sharp features in $G_{||}(B_{||})$. By plotting the $B_{||}$-positions of the features as a function of a surface gate voltage V_G, the gap energy can be extracted.

2. Experimental Set-up

Three MBE-grown structures were studied, each consisting of a modulation-doped pair of GaAs QWs of equal width w separated by an $Al_{0.3}Ga_{0.7}As$ barrier of thickness t. Samples A, B, and C had w=150 Å, t = 25 Å; w = 100 Å, t = 35Å; and w = 150 Å, t =

* Also at Oregon State University, Corvallis, Oregon 97331

This work was supported by the United States Department of Energy under Contract DE-AC04-94AL85000.

15 Å, respectively. Standard four terminal low-frequency lock-in measurements were performed at $T \geq 0.3$ K on 0.2 mm wide Hall bars with Cr/Au surface gates. At V_G=0, samples A, B, and C had top QW densities $n_1 \approx 1.4$, 1.2 and 0.7 x 10^{11} cm^{-2}, and bottom QW densities $n_2 \approx 1.5$, 1.2, and 0.9 x 10^{11} cm^{-2}, respectively. The V_G=0 mobilities of the top QW were $\mu_1 \approx 2.7$, 1.2, and 0.6 x 10^5 cm^2/Vs, and of the bottom QW were $\mu_2 \approx 2.2$, 0.6, and 0.2 x 10^5 cm^2/Vs, respectively. n_1 and n_2 were determined from quantum Hall and Shubnikov-de Haas (SdH) measurements in $B_\perp$, followed by a rotation *in situ* for measurement in $B_\parallel$, with the residual component of $B_\perp$ less than 0.005 T. The applied electric field was nominally parallel to $B_\parallel$.

3. Effect of Anticrossing on the In-Plane Conductance

Fig. 1 shows the normalized $G_\parallel(B_\parallel)$ for several V_G. For V_G=0, a sharp maximum appears at $B_{max} \approx 5.8$ T, followed by a sharp minimum at $B_{min} \approx 6.4$ T. As V_G decreases, both features move to lower $B_\parallel$, with B_{max} moving more rapidly than B_{min}. The features disappear once the top QW depletes at V_G = -0.29 V, since their origin is due solely to interactions between the two QWs. The maximum and minimum correspond respectively to the upper and lower edges of the minigap crossing the Fermi level.

Fig. 2 shows the results of a tight-binding calculation[5] for a double QW structure

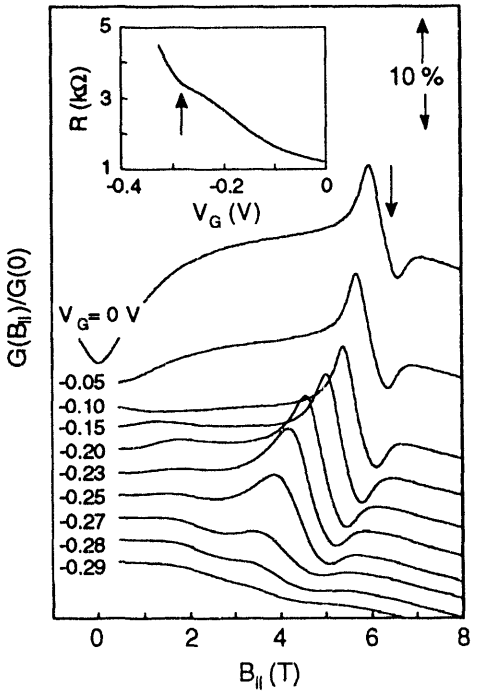

FIG. 1. Normalized $G_\parallel$ vs.$B_\parallel$ of sample A for different V_G, offset from one another by 2 %. Arrow indicates $\hbar(k_1+k_2)/ed$ for V_G=0, with d from a Hartree self-consistent calculation. Inset: $B_\parallel$=0 resistance vs. V_G.

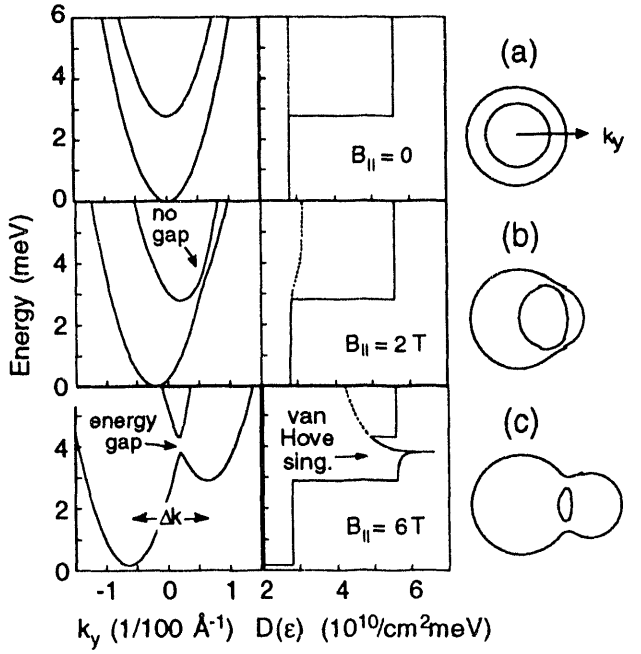

FIG. 2. Calculated dispersion $\varepsilon(k_y)$ (left); calculated density of states $D(E)$ (middle) for lower energy branch (dotted line) and both energy branches (solid line); and sketch of Fermi surface for $\mu \approx 5$ meV (right); for $B_\parallel$ = (a) 0 T, (b) 2 T, and (c) 6 T.

having w = 140 Å, t = 60 Å, and unequal QW depths of 280 and 277 meV. (These parameters, while somewhat different from those of the experiment, illustrate the essential physics nicely.) The left column shows the two lowest eigenenergies $\varepsilon_{\pm}(k_y)$, the middle column the density of states D(E), and the right column a sketch of the Fermi surface for chemical potential μ = 5 meV. The three rows are (a) $B_{||}$ = 0 T, (b) 2 T, and (c) 6 T. At $B_{||}$ = 0 the $\varepsilon_{\pm}(k_y)$ curves are parabolic and $D(E)$ is constant for each energy branch, with the energy splitting mainly due to the unequal QW depths. The other two $B_{||}$ values were chosen so that with no coupling the Fermi circles touch tangentially on the inside and outside, respectively, at the same $\mu \approx 4$ meV. This corresponds to $\Delta k_y = k_1 \pm k_2$, where k_1 and k_2 are the Fermi wavevectors of the top and bottom QWs. When coupling is present, these two cases exhibit two types of anticrossings: In the first, at 2 T, the slopes of $\varepsilon_{\pm}(k_y)$ deviate but do not change sign, changing the group velocity near the anticrossing only slightly. No minigap appears, and the slight changes in $D(E)$ due to each energy branch cancel one another. Thus the effect on $G_{||}$ of this type of anticrossing passing through μ is negligible. This is in accord with the V_G=0 data of Fig. 1, for which no features appear at $B_{||} = \hbar(k_1 - k_2)/ed$ = *XXX*.

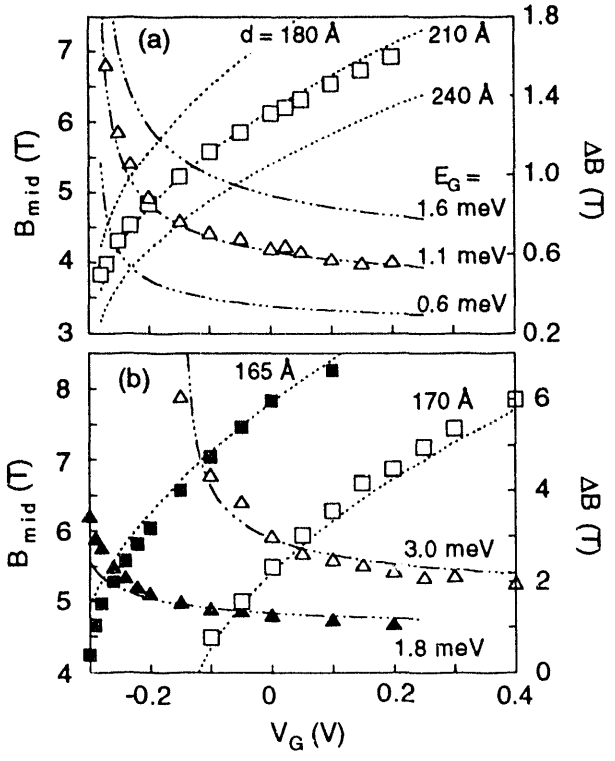

FIG. 3. (a) Plot of B_{mid} (squares) and ΔB (triangles) for sample A. Using sample A parameters, dotted lines are plots of Eq. (1) for various d, while dash-dotted lines are plots of Eq. (2) (using the d obtained from the fit to Eq. 3) for various E_G. (b) Same as in (a), but for samples B (solid symbols) and C (open symbols), and only showing the best fits.

In the second type of anticrossing, at 6 T, the slopes of $\varepsilon_{\pm}(k_y)$ change sign, and a minigap of width E_G appears. E_G is insensitive to $B_{||}$ and $\approx \Delta_{SAS}$, the $B_{||}$=0 symmetric-antisymmetric gap existing when the QW depths (densities) are equal.[5] At the upper gap edge the dispersion is nearly parabolic and a sharp step-like reduction appears in $D(E)$. States at the upper gap edge have low velocities and contribute little current, yet make significant contributions to the scattering rates of electrons elsewhere on the Fermi surface. As $B_{||}$ increases, pushing the upper gap edge through μ, electrons are no longer scattered into these states, yielding a sharp decrease in the scattering rates and producing the observed maximum in $G_{||}$. The lower gap edge, by contrast, has a saddle-shaped dispersion $\varepsilon(k_x,k_y) = \varepsilon_0 + (\hbar k_x)^2/2m^* - (\hbar k_y)^2/2m'$, where ε_0 is the saddle-point energy, and m' is determined by the saddle-point

curvature. This type of dispersion produces a Van Hove singularity at ε_0 of the form $D(E) \propto -\ln(\varepsilon-\varepsilon_0)$. Since the saddle point states have zero group velocity, when $B_{||}$ is swept and the lower gap edge passes through μ, electrons are divergently scattered into states that carry no current, yielding the sharp minimum in $G_{||}$.

4. Gate Bias and Minigap Energy

Negatively biasing the gate causes the features in $G_{||}$ to move to lower $B_{||}$. To a first approximation, V_G linearly changes n_1 while leaving n_2 unchanged. Assuming $B_{mid} = (B_{min}+B_{max})/2$ corresponds to μ lying in mid-gap, or equivalently, to $\hbar(k_1+k_2)/ed$, then

$$B_{mid} = \left(\sqrt{\frac{C_G}{e}(V_G - V_{depl})} + \sqrt{n_2}\right)\frac{\hbar\sqrt{2\pi}}{ed} \qquad (1)$$

where C_G is the calculated gate capacitance and n_2 and V_{depl} are known from measurements in $B_\perp$. In Fig. 3 we show fits of Eq. (1) to the B_{mid} vs V_G data, with d as the only adjustable parameter. Hartree self-consistent calculations (HSCCs) give values for d of 195, 140, and 180 Å for samples A, B, and C, respectively, in relatively good agreement with the data.

As seen in Fig. 1, $\Delta B = B_{min}-B_{max}$ increases as V_G is decreased Using the same model and assuming that B_{max} and B_{min} occur at $\hbar[k_1+k_2\pm(\Delta k_1+\Delta k_2)]/ed$, where $\Delta k_{1,2} = E_G/(2\partial E/\partial k_{1,2})$ and $\partial E/\partial k_{1,2}$ is evaluated as $(2\pi n_{1,2})^{1/2}\hbar^2/m^*$, we obtain

$$\Delta B = \left[\left(\frac{C_G}{e}(V_G - V_{depl})\right)^{-1/2} + n_2^{-1/2}\right]\frac{E_G m^*}{ed\hbar\sqrt{2\pi}} \qquad (2)$$

Fig. 3 shows fits of Eq. (2) to the ΔB data, using the values for d obtained from the fits of Eq. (1). E_G is the only adjustable parameter. The fits yield E_G = 1.1, 1.8, and 3.0 meV for samples A, B, and C, in fair agreement with the values of 1.4, 2.0, and 3.4 meV obtained from HSCCs, and demonstrating that E_G can be directly obtained from the data. The model breaks down as E_G becomes large, so the discrepancy is largest for sample C.

We thank T. R. Castillo for technical assistance. This work was supported by the U.S. Dept. of Energy under Contract DE-AC04-94AL85000.

5. References

1. J. P. Eisenstein *et al.*, Phys. Rev. **B44** (1991) 6511.
2. J. A. Simmons *et al.*, Phys. Rev. **B47** (1993) 15741; S. K. Lyo and J. A. Simmons, J. Phys.: Condens. Matter **5** (1993) L299.
3. While G. S. Boebinger *et al.*, Phys. Rev. B **43**, 12673 (1991) studied Fermi-surface distortions through measurements of $B_{||}$-induced changes in the Shubnikov-de Haas oscillations in a $B_\perp$, the $B_{||}$ component was too small to produce an anticrossing-type energy gap, and $G_{||}(B_{||})$ for $B_\perp$=0 was not investigated.
4. Many years ago vicinal planes of Si were shown to have a similarly shaped Fermi surface arising by an entirely different mechanism, intervally coupling. See D. C.

Tsui *et al.*, Phys. Rev. Lett. **25** (1978) 1667, T. Ando, Phys. Rev. **B19**, (1979) 3089, and references therein.
5. S. K. Lyo, unpublished.

DISCLAIMER

II

DATE FILMED

8/23/94

END